Ingeniería y Competitividad
Vol 28 (2) 2026 doi: 10.25100/iyc.v28i2.15590

Vol 28 (2)

ISSN
0123-3033
e- 2027-8284

Original Article

Bidirectional Canonical Model for a Cascaded Buck-Boost DC/DC Converter

Modelo canónico bidireccional para un convertidor CC/CC Buck-Boost en cascada

María Alejandra Mantilla Villalobos[1] Oscar Olarte Ortiz[1] Fausto Osorio Silva[1]
Javier Enrique Solano Martínez[1]

[1] Universidad Industrial de Santander. Bucaramanga, Colombia.

Abstract

Introduction: Bidirectional DC/DC converters facilitate energy management in applications like electric vehicles featuring regenerative braking. Controller design for these systems relies on dynamic models offering lower computational demands compared to full switched representations. This study derives steady-state averaged (DC) and small-signal dynamic (AC) models for the cascaded bidirectional buck-boost converter operating in continuous conduction mode across its four defined states.
Objective: The primary objective is to develop a unified canonical bidirectional model capable of representing the cascaded buck-boost converter dynamics through a single standard structure for all operating modes.
Methods: Dynamic equations for the four operating modes were derived applying state-space averaging, perturbation, and linearization techniques, subsequently implementing the canonical model in the MATLAB/Simulink environment.
Results: A unified bidirectional canonical circuit model was developed for controller design. Validation was achieved by comparing its dynamic response to step changes in input voltage with a switched circuit model.
Conclusions: The proposed model is a tool that represents all four operating modes of the converter with a unified circuit structure, avoiding the use of separate models for each power flow and operating mode. This facilitates dynamic system analysis and design control strategies by providing a linearized model suitable for classical and advanced controllers. Furthermore, the model is particularly useful in applications involving charging and discharging energy storage systems, such as electric vehicles, because it describes the behavior of the converter under bidirectional power flow.

Keywords: Cascaded buck-boost bidirectional converter, canonical model, state-space averaging method, small-signal AC model

Resumen

Introducción: Los convertidores CC/CC bidireccionales facilitan la gestión de la energía en aplicaciones como los vehículos eléctricos con frenado regenerativo. El diseño de controladores para estos sistemas se basa en modelos dinámicos que ofrecen menores exigencias computacionales en comparación con las representaciones conmutadas completas. Este estudio deriva modelos promediados en estado estacionario (CC) y dinámicos de pequeña señal (CA) para el convertidor elevador-reductor bidireccional en cascada que opera en modo de conducción continua a través de sus cuatro estados definidos.
Objetivo: El objetivo principal es desarrollar un modelo bidireccional canónico unificado capaz de representar la dinámica del convertidor elevador-reductor en cascada mediante una única estructura estándar para todos los modos de operación.
Métodos: Se derivaron ecuaciones dinámicas para los cuatro modos de operación aplicando técnicas de promediado en el espacio de estados, perturbación y linealización, implementando posteriormente el modelo canónico en el entorno MATLAB/Simulink.
Resultados: Se desarrolló un modelo de circuito canónico bidireccional unificado para el diseño del controlador. La validación se logró comparando su respuesta dinámica a cambios escalonados en la tensión de entrada con un modelo de circuito conmutado.
Conclusiones: El modelo propuesto es una herramienta que representa los cuatro modos de operación del convertidor con una estructura de circuito unificada, evitando el uso de modelos separados para cada flujo de potencia y modo de operación. Esto facilita el análisis dinámico del sistema y el diseño de estrategias de control al proporcionar un modelo linealizado adecuado para controladores clásicos y avanzados. Además, el modelo es particularmente útil en aplicaciones que involucran sistemas de almacenamiento de energía de carga y descarga, como vehículos eléctricos, ya que describe el comportamiento del convertidor bajo flujo de potencia bidireccional.

Palabras clave: Convertidor bidireccional elevador-reductor en cascada, modelo canónico, método de promediado en el espacio de estados, modelo de CA de pequeña señal.

How to cite?

Mantilla MA, Olarte O, Osorio F, Solano JE. Bidirectional Canonical Model for a Cascaded Buck-Boost DC/DC Converter Ingeniería y Competitividad, 2026, 28(2) e-20715590

https://doi.org/10.25100/iyc.v28i2.15190

Received: 26/01/26
Reviewed: 28/04/26
Accepted: 05/06/26
Online: /05/26

Correspondence

marialem@uis.edu.co

Spanish version

Why was this study conducted?
The inherent nonlinear and time-varying nature of bidirectional DC/DC converters complicates controller design using complete switched models, necessitating linearized representations for electric mobility applications featuring regenerative braking. Current literature provides canonical models for traditional topologies but lacks a unified representation for the cascaded bidirectional buck-boost converter across its four operating modes. This study develops and validates a unified bidirectional canonical model to represent the converter dynamics in a standard format.

What were the most relevant findings?
Using the state-space averaging method and small-signal linearization, the dynamic behavior of the four converter operating modes (Buck1-2, Boost1-2, Buck2-1, and Boost2-1) was condensed into a single standard equivalent circuit. MATLAB/Simulink simulations validated this representation, demonstrating that its dynamic response to disturbances, such as step changes in the input voltage, matches the traditional switched model. The proposed model tracks the average signal values and eliminates the high-frequency ripple while preserving the underlying system dynamics.

What do these findings contribute to?
The canonical model standardizes the engineering process by enabling the application of classical linear control techniques for feedback controller design. Unifying the four operating modes into a single representation streamlines the stability analysis and the development of energy management systems for electric mobility applications featuring regenerative braking.

Graphical Abstract

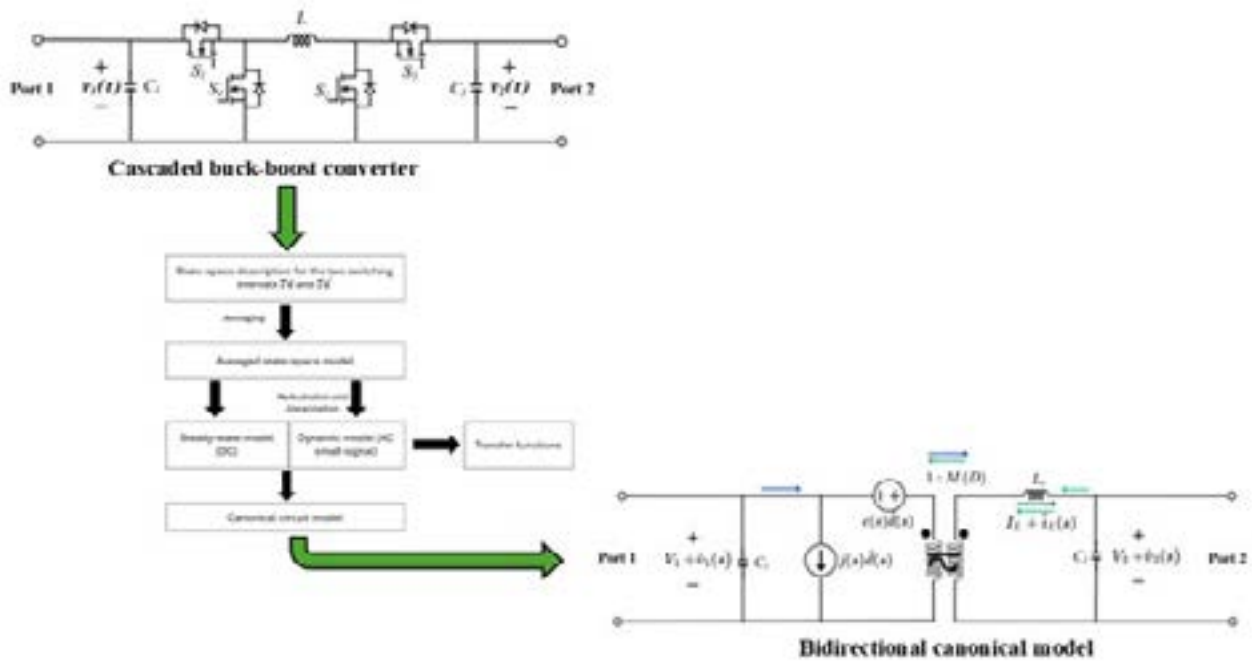

doi: 10.25100/iyc.v28i2.15590

Introduction

The environmental impact of ground transportation, which is responsible for a significant portion of CO_2 emissions (1–3), has driven the search for more environmentally friendly alternatives. Electric vehicles (EV) have emerged as a solution, although their carbon footprint depends on the energy mix (4). In this context, electric bicycles (EB) are gaining prominence as they are environmentally superior to other motorized means of transportation (5,6).

In addition, the electric mobility paradigm has evolved beyond simple transportation. Currently, electric vehicles are integrated into Smart Grids under concepts such as vehicle-to-grid (V2G) and vehicle-to-home (V2H), where bidirectional energy flow is a desired operational capability (7,8). This functionality enables traction and support for the electrical grid and energy demand management, which require highly efficient and versatile power conversion stages (9).

A feature that optimizes the efficiency of these vehicles is their energy recovery capability. The potential for regenerative braking is considerable in steep topographies. However, most commercial systems do not allow bidirectional energy flow. Bidirectional DC/DC power converters are required to implement regenerative braking (10–12).

The cascaded Buck-Boost converter, frequently designated as the non-inverting buck-boost converter, maintains a prominent status in recent literature compared to topologies such as Cuk, SEPIC, or Zeta (13). This configuration provides an extended voltage conversion range without inverting the output polarity, while imposing lower voltage stress on the power switches (14,15). Recent research identifies its suitability for hybrid storage systems incorporating fuel cells, batteries, and supercapacitors where DC bus stability remains a primary design constraint (16).

Designing robust controllers for these systems involves managing inherently nonlinear and time-varying dynamics. Although advanced control strategies, such as Model Predictive Control (MPC) (17) and Sliding Mode Control (SMC) (18), demonstrate superior dynamic performance, their implementation often requires high computational resources. Consequently, industrial applications favor classical linear control techniques (PI/PID) for their simplicity and reliability, provided that an accurate dynamic model exists (19).

Developing equivalent small-signal linear models satisfies standard design specifications for linear control (20). The state-space averaging method focuses on system dynamics by neglecting high-frequency components arising from transistor switching (21). While researchers propose various modeling approaches based on signal flow graphs (22) and current injection techniques (23), many resulting expressions possess high mathematical complexity, hindering the physical insight necessary for controller design.

Existing literature contains canonical model proposals for traditional topologies (24,25) and small-signal analyses for quadratic or multilevel converters (26,27). However, the reviewed literature lacks documentation on a canonical circuit model specific to the cascaded bidirectional DC/DC buck-boost converter covering its four operating modes under a single standard structure (28).

This study presents a canonical bidirectional model for a cascaded DC/DC buck-boost converter, considering its four operating modes. The objective was to develop a unified linearized model that

doi: 10.25100/iyc.v28i2.15590

facilitates control design. The proposed model was implemented and validated through a simulation in MATLAB/Simulink, and its dynamic response was compared with traditional switched model to verify its accuracy.

Methodology (Converter Modeling)

For the control system design of DC/DC converters, an input-output mathematical model is required to approximate physical reality. The converters are nonlinear and time-varying systems, and there is interest in developing an equivalent small-signal linear model, through which it becomes possible to design a feedback controller using linear control techniques (20).

The topology selected for this study was a cascaded bidirectional buck-boost converter, as shown in Figure 1. This bidirectional converter features four modes of operation. The low-frequency dynamic behaviors can be represented using the small-signal model described for each mode. To define a general equivalent circuit model that enables the operation of all four converter modes to be described, the models for each mode are adapted to the canonical circuit model form, resulting in a unified bidirectional circuit model that allows the converter behavior to be represented in any of its four modes.

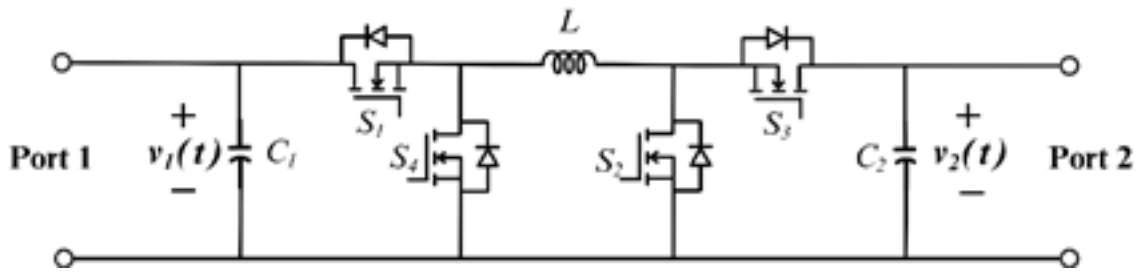

Figure 1 . Buck - Boost cascaded converter

Modeling Method

The power converter was modeled using the state-space averaging method. This method, described in detail by (21,29), allows for the derivation of the steady-state averaged model (DC) and the small-signal dynamic model (AC) for switched converters operating in continuous conduction mode. The process, as shown in Figure 2, consists of the following steps:

1. Obtain the state-space description for each switching interval of the converter.
2. The descriptions are averaged over a switching period to obtain an average state-space model that describes the low frequency dynamics.
3. The averaged model is perturbed and linearized at a quiescent operating point.
4. Convert the model to the frequency domain (s-domain) to obtain the transfer functions.
5. The resulting model is adapted to the canonical form.

doi: 10.25100/iyc.v28i2.15590

The process described above was performed for the four operating modes of the cascaded bidirectional buck-boost converter under study.

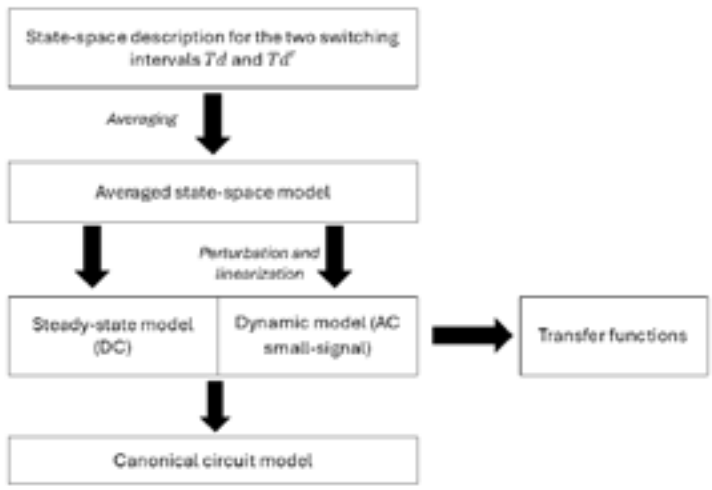

Figure 2. Steps for modeling the power stage - Adapted from (21,29)

Modes of Operation and Switched Modeling

The cascaded bidirectional buck-boost converter features four possible modes of operation, defined in Table 1. The $Buck_{1-2}$ and $Boost_{1-2}$ modes consider Port 1 as the input and Port 2 as the output, performing step-down and step-up functionalities, respectively. The $Buck_{2-1}$ and $Boost_{2-1}$ modes operate in the opposite direction (regenerative braking), with Port 2 as the input and Port 1 as the output, and function in the step-down and step-up modes (input-output relationship), respectively.

The converter contains four controlled power electronic devices (power transistors), denoted as S_1, S_2, S_3, and S_4. Depending on the converter's operating mode, these devices are controlled, as indicated in Table 1. For each mode, only one of the four transistors is periodically controlled or switched, whereas the other three transistors remain in their active (1) or inactive (0) states.

Table 1 . Operating modes of the cascaded buck-boost converter

Mode	p	S_1	S_2	S_3	S_4
$Buck_{1-2}$	1	Controlled	0	0	0
$Boost_{1-2}$	2	1	Controlled	0	0
$Buck_{2-1}$	3	0	0	Controlled	0
$Boost_{2-1}$	4	0	0	1	Controlled

Assuming continuous conduction mode, that is, the instantaneous current through the inductor does not drop to zero at any point in the cycle, in each mode of operation, the converter can be modeled by two equivalent circuits for the switching intervals Td (the interval in which the controlled transistor is in the active state) and Td' (the interval in which the controlled transistor is in the inactive state), where T is the converter's switching period, d is the duty cycle, and d' = (1 –

doi: 10.25100/iyc.v28i2.15590

d). The resulting circuits are shown in Figure 3. For the $Buck_{1\text{-}2}$ and $Boost_{1\text{-}2}$ modes, an independent voltage source $v_1(t)$ is connected to Port 1, and a load resistor R_2 is connected to Port 2. Similarly, for the $Buck_{2\text{-}1}$ and $Boost_{2\text{-}1}$ modes, an independent voltage source $v_2(t)$ is connected to Port 2 and a load resistor R_1 to Port 1. These assumptions are consistent with the energy flow and operation of the converter according to its operating mode.

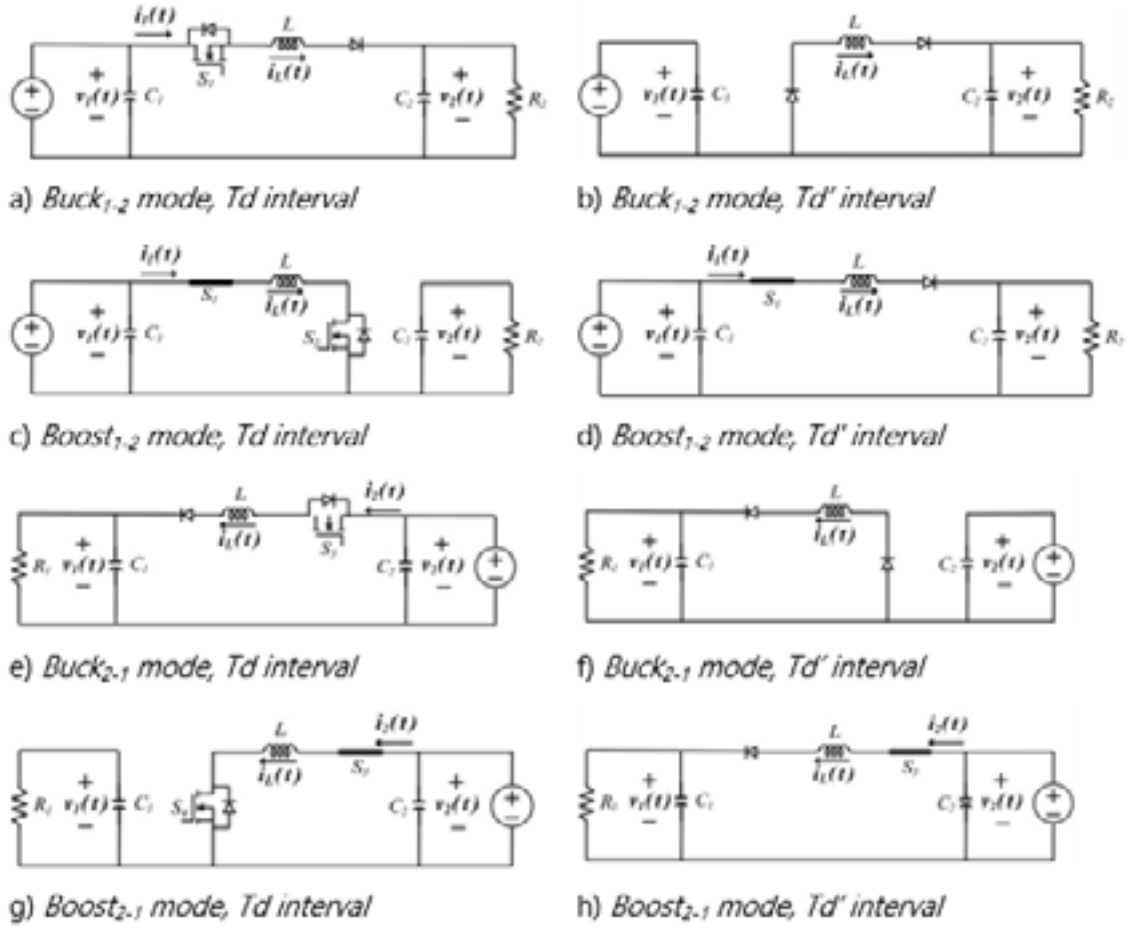

Figure 3. Equivalent circuits for each operating mode of the cascaded buck-boost converter

Based on these circuits, the switched state-space dynamic model is derived for each subinterval (Td and Td') and expressed in general form in equations (1), (2), (3):

$$\boldsymbol{K}_p \frac{d\boldsymbol{x}_p(t)}{dt} - \boldsymbol{A}_{p,q}\boldsymbol{x}_p(t) + \boldsymbol{B}_{p,q}\boldsymbol{u}_p(t) \tag{1}$$

$$\boldsymbol{y}_p(t) = \boldsymbol{E}_{p,q}\boldsymbol{x}_p(t) + \boldsymbol{F}_{p,q}\boldsymbol{u}_p(t) \tag{2}$$

$$p \in \{1,2,3,4\}; \quad q \in \{0,1\} \tag{3}$$

doi: 10.25100/iyc.v28i2.15590

where $x_p(t)$ corresponds to the state vector, $u_p(t)$ to the input vector, $y_p(t)$ to the output vector, p indicates the operating mode according to Table 1, and q represents the logic switching signal, with q = 1, the controlled transistor is active (subinterval Td), and q = 0, the transistor is inactive (subinterval Td'). Table 2 summarizes the resulting vectors and matrices for each equivalent circuit.

Table 2. Vectors and matrices for the switched-state-space dynamic models of the cascaded buck-boost converter

	Buck$_{1\text{-}2}$ (p=1)	Boost$_{1\text{-}2}$ (p=2)	Buck$_{2\text{-}1}$ (p=3)	Boost$_{2\text{-}1}$ (p=4)
$x_p(t)$	$\begin{bmatrix} i_L(t) \\ v_2(t) \end{bmatrix}$	$\begin{bmatrix} i_L(t) \\ v_2(t) \end{bmatrix}$	$\begin{bmatrix} i_L(t) \\ v_1(t) \end{bmatrix}$	$\begin{bmatrix} i_L(t) \\ v_1(t) \end{bmatrix}$
$u_p(t)$	$v_1(t)$	$v_1(t)$	$v_2(t)$	$v_2(t)$
$y_p(t)$	$i_1(t)$	$i_1(t)$	$i_2(t)$	$i_2(t)$
K_p	$\begin{bmatrix} L & 0 \\ 0 & C_2 \end{bmatrix}$	$\begin{bmatrix} L & 0 \\ 0 & C_2 \end{bmatrix}$	$\begin{bmatrix} L & 0 \\ 0 & C_1 \end{bmatrix}$	$\begin{bmatrix} L & 0 \\ 0 & C_1 \end{bmatrix}$
$A_{p,1}$	$\begin{bmatrix} 0 & -1 \\ 1 & -\frac{1}{R_2} \end{bmatrix}$	$\begin{bmatrix} 0 & 0 \\ 0 & -\frac{1}{R_2} \end{bmatrix}$	$\begin{bmatrix} 0 & -1 \\ 1 & -\frac{1}{R_1} \end{bmatrix}$	$\begin{bmatrix} 0 & 0 \\ 0 & -\frac{1}{R_1} \end{bmatrix}$
$A_{p,0}$	$\begin{bmatrix} 0 & -1 \\ 1 & -\frac{1}{R_2} \end{bmatrix}$	$\begin{bmatrix} 0 & -1 \\ 1 & -\frac{1}{R_2} \end{bmatrix}$	$\begin{bmatrix} 0 & -1 \\ 1 & -\frac{1}{R_1} \end{bmatrix}$	$\begin{bmatrix} 0 & -1 \\ 1 & -\frac{1}{R_1} \end{bmatrix}$
$B_{p,1}$	$\begin{bmatrix} 1 \\ 0 \end{bmatrix}$	$\begin{bmatrix} 1 \\ 0 \end{bmatrix}$	$\begin{bmatrix} 1 \\ 0 \end{bmatrix}$	$\begin{bmatrix} 1 \\ 0 \end{bmatrix}$
$B_{p,0}$	$\begin{bmatrix} 0 \\ 0 \end{bmatrix}$	$\begin{bmatrix} 1 \\ 0 \end{bmatrix}$	$\begin{bmatrix} 0 \\ 0 \end{bmatrix}$	$\begin{bmatrix} 1 \\ 0 \end{bmatrix}$
$E_{p,1}$	$[1\ 0]$	$[1\ 0]$	$[1\ 0]$	$[1\ 0]$
$E_{p,0}$	$[0\ 0]$	$[1\ 0]$	$[0\ 0]$	$[1\ 0]$
$F_{p,1}$	$[0]$	$[0]$	$[0]$	$[0]$
$F_{p,0}$	$[0]$	$[0]$	$[0]$	$[0]$

State-Space Averaged Model

Following the state-space averaging method, the two switched models are averaged over a switching period T, and the natural frequency and converter input frequencies are assumed to be much smaller than the switching frequency.

The average state vector over period T is defined as equation (4).

$$\langle x_p(t) \rangle_T = \frac{1}{T} \int_{t-T/2}^{t+T/2} x_p(\tau) d\tau \qquad (4)$$

doi: 10.25100/iyc.v28i2.15590

This operation allows the low-frequency components of the state vector to be modeled. The same operation is performed on the input vectors $\boldsymbol{u_p}(t)$ and output $\boldsymbol{y_p}(t)$. By averaging the descriptions of the switched models over one switching period, the averaged state-space model is presented in equations (5) and (6).

$$\boldsymbol{K_p}\frac{d\langle \boldsymbol{x_p}(t)\rangle_T}{dt} - \left(d(t)\boldsymbol{A_{p,1}} + d'(t)\boldsymbol{A_{p,0}}\right)\langle \boldsymbol{x_p}(t)\rangle_T + \left(d(t)\boldsymbol{B_{p,1}} + d'(t)\boldsymbol{B_{p,0}}\right)\langle \boldsymbol{u_p}(t)\rangle_T \quad (5)$$

$$\langle \boldsymbol{y_p}(t)\rangle_T = \left(d(t)\boldsymbol{E_{p,1}} + d'(t)\boldsymbol{E_{p,0}}\right)\langle \boldsymbol{x_p}(t)\rangle_T + \left(d(t)\boldsymbol{F_{p,1}} + d'(t)\boldsymbol{F_{p,0}}\right)\langle \boldsymbol{u_p}(t)\rangle_T \quad (6)$$

Steady-state solution

If the duty cycle remains constant from cycle to cycle, that is, d(t) = D (steady-state DC duty cycle), and a direct current input $\boldsymbol{u_p}(t) = \boldsymbol{U_p}$ is applied, the converter operates in equilibrium when the derivatives of all elements of vector $\langle \boldsymbol{x_p}(t)\rangle_T$ are zero. Thus, the steady-state (DC) model that describes the converter in equilibrium is given by equations (7) and (8) (21):

$$\boldsymbol{0} = \boldsymbol{A_p}\boldsymbol{X_p} + \boldsymbol{B_p}\boldsymbol{U_p} \quad (7)$$

$$\boldsymbol{Y_p} = \boldsymbol{E_p}\boldsymbol{X_p} + \boldsymbol{F_p}\boldsymbol{U_p} \quad (8)$$

where the resulting averaged matrices for D′ = 1 - D, are given by equations (9) to (12):

$$\boldsymbol{A_p} = D\boldsymbol{A_{p,1}} + D'\boldsymbol{A_{p,0}} \quad (9)$$

$$\boldsymbol{B_p} = D\boldsymbol{B_{p,1}} + D'\boldsymbol{B_{p,0}} \quad (10)$$

$$\boldsymbol{E_p} = D\boldsymbol{E_{p,1}} + D'\boldsymbol{E_{p,0}} \quad (11)$$

$$\boldsymbol{F_p} = D\boldsymbol{F_{p,1}} + D'\boldsymbol{F_{p,0}} \quad (12)$$

The equilibrium values (DC) of the average vectors can be obtained from equations (13) and (14):

$$\boldsymbol{X_p} = -\boldsymbol{A_p^{-1}}\boldsymbol{B_p}\boldsymbol{U_p} \quad (13)$$

$$\boldsymbol{Y_p} = \left(-\boldsymbol{E_p}\boldsymbol{A_p^{-1}}\boldsymbol{B_p} + \boldsymbol{F_p}\right)\boldsymbol{U_p} \quad (14)$$

Carrying out the above procedure for the four operating modes of the converter under study yields the steady-state (DC) solution, and the average matrices are presented in Table 3.

doi: 10.25100/iyc.v28i2.15590

Table 3. Steady-state (DC) solution and resulting matrices for the averaged state-space models of the cascaded buck–boost converter

	$\text{Buck}_{1\text{-}2}$ (p=1)	$\text{Boost}_{1\text{-}2}$ (p=2)	$\text{Buck}_{2\text{-}1}$ (p=3)	$\text{Boost}_{2\text{-}1}$ (p=4)
X_p	$\begin{bmatrix} I_L \\ V_2 \end{bmatrix} = \begin{bmatrix} \frac{DV_1}{R_2} \\ DV_1 \end{bmatrix}$	$\begin{bmatrix} I_L \\ V_2 \end{bmatrix} = \begin{bmatrix} \frac{V_2^2}{V_1 R_2} \\ \frac{V_1}{D'} \end{bmatrix}$	$\begin{bmatrix} I_L \\ V_1 \end{bmatrix} = \begin{bmatrix} \frac{DV_2}{R_1} \\ DV_2 \end{bmatrix}$	$\begin{bmatrix} I_L \\ V_1 \end{bmatrix} = \begin{bmatrix} \frac{V_1^2}{V_2 R_1} \\ \frac{V_2}{D'} \end{bmatrix}$
U_p	V_1	V_1	V_2	V_2
Y_p	$I_1 - DI_L$	$I_1 - I_L$	$I_2 - DI_L$	$I_2 - I_L$
K_p	$\begin{bmatrix} L & 0 \\ 0 & C_2 \end{bmatrix}$	$\begin{bmatrix} L & 0 \\ 0 & C_2 \end{bmatrix}$	$\begin{bmatrix} L & 0 \\ 0 & C_1 \end{bmatrix}$	$\begin{bmatrix} L & 0 \\ 0 & C_1 \end{bmatrix}$
A_p	$\begin{bmatrix} 0 & -1 \\ 1 & -\frac{1}{R_2} \end{bmatrix}$	$\begin{bmatrix} 0 & -D' \\ D' & -\frac{1}{R_2} \end{bmatrix}$	$\begin{bmatrix} 0 & -1 \\ 1 & -\frac{1}{R_1} \end{bmatrix}$	$\begin{bmatrix} 0 & -D' \\ D' & -\frac{1}{R_1} \end{bmatrix}$
B_p	$\begin{bmatrix} D \\ 0 \end{bmatrix}$	$\begin{bmatrix} 1 \\ 0 \end{bmatrix}$	$\begin{bmatrix} D \\ 0 \end{bmatrix}$	$\begin{bmatrix} 1 \\ 0 \end{bmatrix}$
E_p	$[D\ 0]$	$[1\ 0]$	$[D\ 0]$	$[1\ 0]$
F_p	$[0]$	$[0]$	$[0]$	$[0]$

Small-signal AC dynamic model

Small AC variations are introduced, $\hat{x}_p(t)$, $\hat{u}_p(t)$, $\hat{y}_p(t)$ and $\hat{d}(t)$, around the equilibrium operating point for the state vector, input vector, output vector, and duty cycle, respectively, as defined in equations (15)–(18) (21):

$$\langle x_p(t)\rangle_T = X_p + \bar{x}_p(t) \tag{15}$$

$$\langle u_p(t)\rangle_T = U_p + \bar{u}_p(t) \tag{16}$$

$$\langle y_p(t)\rangle_T = Y_p + \bar{y}_p(t) \tag{17}$$

$$d(t) = D + \hat{d}(t) \Rightarrow d'(t) = D' - \hat{d}(t) \tag{18}$$

The average model incorporates these expressions into state-space equations (5) and (6). By expanding the resulting expression, the DC terms (steady state), first-order linear AC terms, and second-order nonlinear terms can be separated. If the small AC variations are substantially smaller than the equilibrium (DC) values, the second-order nonlinear terms are neglected, yielding the linearized small-signal AC model, as represented by equations (19) and (20) (21).

$$K_p \frac{d\hat{x}_p(t)}{dt} = A_p \hat{x}_p(t) + B_p \hat{u}_p(t) + \left[(A_{p,1} - A_{p,0})X_p + (B_{p,1} - B_{p,0})U_p\right]\hat{d}(t) \tag{19}$$

doi: 10.25100/iyc.v28i2.15590

$$\bar{y}_p(t) - E_p\bar{x}_p(t) + F_p\bar{u}_p(t) + [(E_{p.1} - E_{p.0})X_p + (F_{p.1} - F_{p.0})U_p]\hat{d}(t) \quad (20)$$

Inserting the matrix and vector elements from Tables 2 and 3 yields the resulting small-signal AC models for the four operating modes of the cascaded buck–boost converter. The models obtained after simplifying the resulting state-space equations for the four operating modes of the converter are presented below. The small-signal AC model equations for $Buck_{1\text{-}2}$ are presented in equations (21)–(23), and their circuit representation is shown in Figure 4.

$$L\frac{d\hat{i}_L(t)}{dt} = D\hat{v}_1(t) + V_1\hat{d}(t) - \hat{v}_2(t) \quad (21)$$

$$C_2\frac{d\hat{v}_2(t)}{dt} = \hat{i}_L(t) - \frac{\hat{v}_2(t)}{R_2} \quad (22)$$

$$\hat{i}_1(t) = D\hat{i}_L(t) + I_L\hat{d}(t) \quad (23)$$

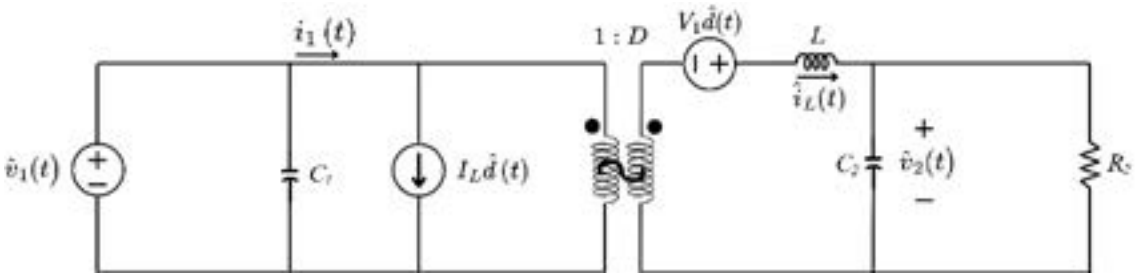

Figure 4. Small-signal AC model for $Buck_{1\text{-}2}$ mode of operation

For the $Boost_{1\text{-}2}$ operating mode, the resulting small-signal AC model equations are presented in (24)–(26), and their circuit representation is shown in Figure 5.

$$L\frac{d\hat{i}_L(t)}{dt} = -D'\hat{v}_2(t) + \hat{v}_1(t) + V_2\hat{d}(t) \quad (24)$$

$$C_2\frac{d\hat{v}_2(t)}{dt} = D'\hat{i}_L(t) - \frac{\hat{v}_2(t)}{R_2} - I_L\hat{d}(t) \quad (25)$$

$$\hat{i}_1(t) = \hat{i}_L(t) \quad (26)$$

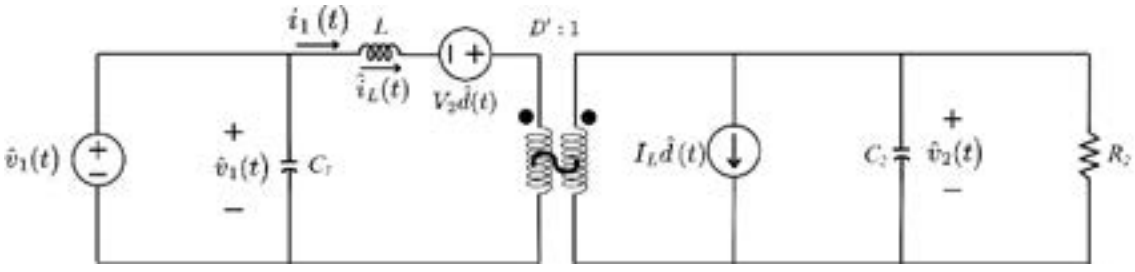

Figure 5. Small-signal AC model for $Boost_{1\text{-}2}$ mode of operation

For the $Buck_{2\text{-}1}$ mode, the small-signal AC model is given by equations (27)–(29) and is shown in Figure 6.

doi: 10.25100/iyc.v28i2.15590

$$L\frac{d\hat{i}_L(t)}{dt} = D\hat{v}_2(t) + V_2\hat{d}(t) - \hat{v}_1(t) \quad (27)$$

$$C_1\frac{d\hat{v}_1(t)}{dt} = \hat{i}_L(t) - \frac{\hat{v}_1(t)}{R_1} \quad (28)$$

$$\hat{i}_2(t) = D\hat{i}_L(t) + I_L\hat{d}(t) \quad (29)$$

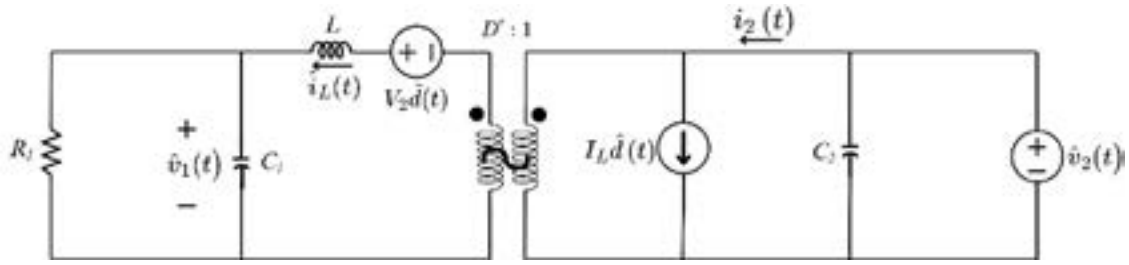

Figure 6. Small-signal AC model for Buck$_{2\text{-}1}$ mode of operation

Finally, for the Boost$_{2\text{-}1}$ mode, the small-signal AC model equations are presented in (30)–(32), and the corresponding circuit is shown in Figure 7.

$$L\frac{d\hat{i}_L(t)}{dt} = -D'\hat{v}_1(t) + \hat{v}_2(t) - V_1\hat{d}(t) \quad (30)$$

$$C_1\frac{d\hat{v}_1(t)}{dt} = D'\hat{i}_L(t) - \frac{\hat{v}_1(t)}{R_1} - I_L\hat{d}(t) \quad (31)$$

$$\hat{i}_2(t) = \hat{i}_L(t) \quad (32)$$

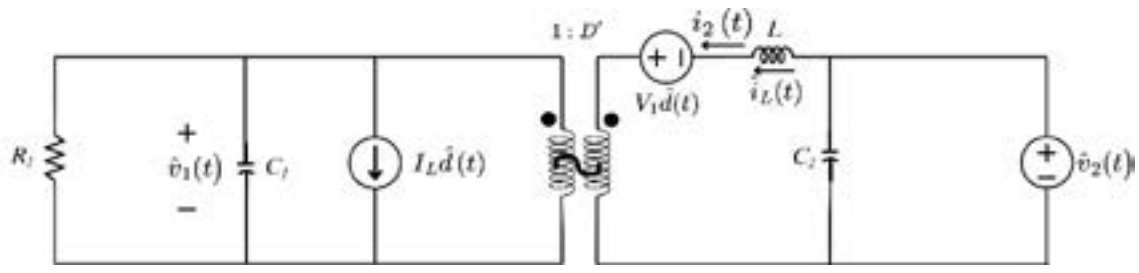

Figure 7. This set of four small-signal linear AC models is the basis for generalization in the bidirectional canonical model.

Bidirectional Canonical Model

The models derived in the previous section for the four operating modes can be mathematically manipulated and generalized into a canonical form. A canonical circuit, such as the one presented in (21), allows for the analysis of the converter's behavior in general terms, without reference to a specific topology. This study proposes a simplification and unification of the four models derived in the previous section into a single **Bidirectional Canonical Model**, as shown in Figure 8. The resulting models for each mode of operation were adapted to the structure of the canonical circuit model by changing the location of certain elements, resulting in a unified bidirectional circuit model that enables the representation of the converter's behavior in any of its four modes. The parameters

doi: 10.25100/iyc.v28i2.15590

of the canonical model, M(D), L_e, e(s), and j(s), resulting from each mode are defined in Table 4.

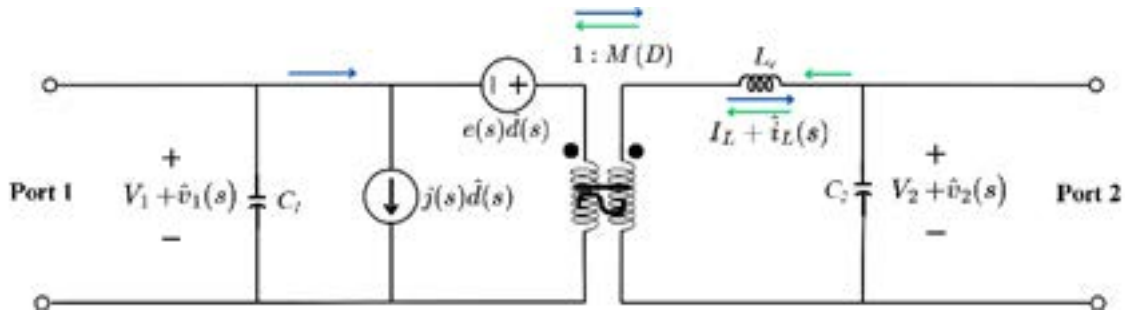

Figure 8. Bidirectional Canonical Model

In the canonical model shown in Figure 8, the blue arrows indicate the direction of the energy flow and currents for the $Buck_{1\text{-}2}$ and $Boost_{1\text{-}2}$ operating modes, whereas the green arrows correspond to the $Buck_{2\text{-}1}$ and $Boost_{2\text{-}1}$ operating modes. Likewise, in the $Buck_{1\text{-}2}$ and $Boost_{1\text{-}2}$ modes, load resistance R_2 is assumed to be connected to Port 2 of the converter, whereas for the $Buck_{2\text{-}1}$ and $Boost_{2\text{-}1}$ modes, load resistance R_1 is assumed at Port 1.

Table 4. Canonical model parameters for the four operating modes of the cascaded buck–boost converter

Mode	$M(D)$	L_e	$e(s)$	$j(s)$
$Buck_{1\text{-}2}$	D	L	$\frac{V_2}{D^2}$	$\frac{V_2}{R_2}$
$Boost_{1\text{-}2}$	$\frac{1}{D'}$	$\frac{L}{D'^2}$	$V_2\left(1-\frac{sL}{D'^2R_2}\right)$	$\frac{V_2}{D'^2R_2}$
$Buck_{2\text{-}1}$	$\frac{1}{D}$	$\frac{L}{D^2}$	$-\frac{V_1}{D}\left(1+\frac{sL}{R_1}\right)$	$\frac{V_1}{DR_1}$
$Boost_{2\text{-}1}$	D'	L	$-\frac{V_1}{D'}$	$\frac{V_1}{D'R_1}$

Simulation Results

To verify the bidirectional canonical model approximates the converter behavior, a simulation was performed. The canonical (averaged) model response was compared with the traditional switched model.

Both models were implemented in the MATLAB/Simulink software. The traditional switched model, depicted in Figure 9, uses power semiconductor elements, specifically transistors and diodes, which are modeled as ideal devices. The switched model, implemented using electrical and electronic components, functions as the equivalent of a virtualized physical circuit for validation. Figure 10 illustrates the canonical bidirectional model implemented in MATLAB/Simulink.

doi: 10.25100/iyc.v28i2.15590

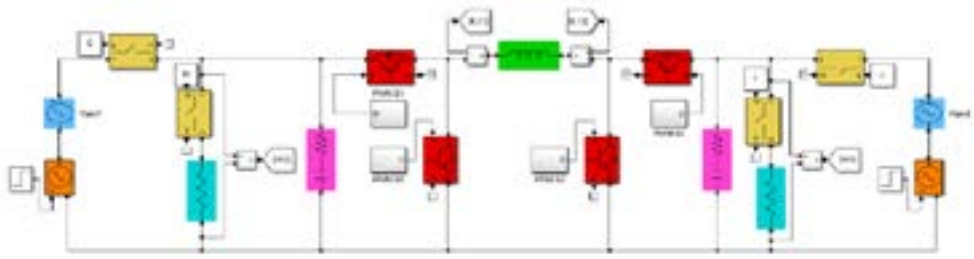

Figure 9. Simulation model of the traditional switched converter in MatLab/Simulink

In Figures 9 and 10, the DC input sources are represented by orange dependent sources. The small-signal AC variations in the input voltage are represented by independent sources in light blue. The load considered was purely resistive and connected according to the mode of operation. Ideal yellow switches are used to disconnect and connect different elements (input sources and loads) according to the operating mode to be evaluated.

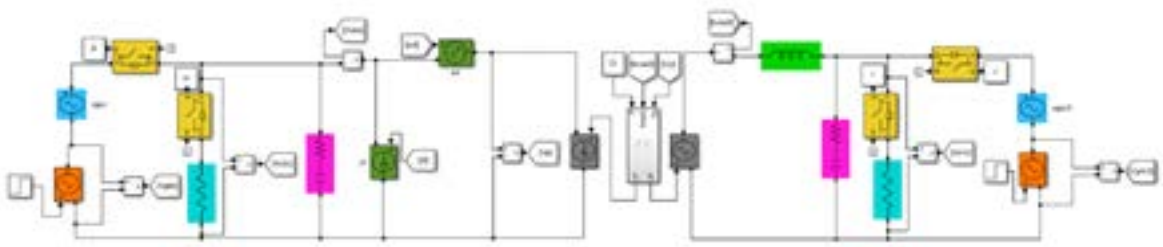

Figure 10. Bidirectional canonical model implemented in MatLab/Simulink

The simultaneous simulation of both models (the canonical circuit and the traditional switched model) was performed using the same parameters and values, which are summarized in Table 5. To assess the accuracy of the canonical model under dynamic changes, the simulation included a change in the amplitude of the DC input voltage at t = 50 ms.

Table 5. Simulation parameters

Parameter	$Boost_{1-2}$	$Buck_{2-1}$
D	0.5	0.5
Amplitude $\hat{d}(t)$	0.01	0.01
Frequency $\hat{d}(t)$	1 (kHz)	1 (kHz)
Initial DC input source ($0 \leq t < 50\ ms$)	$V_1 = 12\ (V)$	$V_2 = 36\ (V)$
Final DC input source ($50 \leq t < 100\ ms$)	$V_1 = 18\ (V)$	$V_2 = 48\ (V)$
Amplitude of the input voltage AC variations	1 (V)	1 (V)
Frequency of the input voltage AC variations	500 (Hz)	500 (Hz)
L	600 (µH)	600 (µH)
C_1	500 (µF)	500 (µF)
C_2	500 (µF)	500 (µF)
Resistive load	$R_2 = 4\ \Omega$	$R_1 = 4\ \Omega$
Switching frequency	20 (kHz)	20 (kHz)

doi: 10.25100/iyc.v28i2.15590

The results for the $Boost_{1-2}$ operating mode are presented in Figure 11 and 12, including a close-up of the instant at which the change in the power-supply amplitude occurs. Figure 11 compares the output voltages of the two models under study. The response of the averaged model ("V2 Averaged") follows the mean value of the switched signal ("V2 Switched"), eliminating the high-frequency ripple. The same behavior was observed for the inductor current as shown in Figure 12.

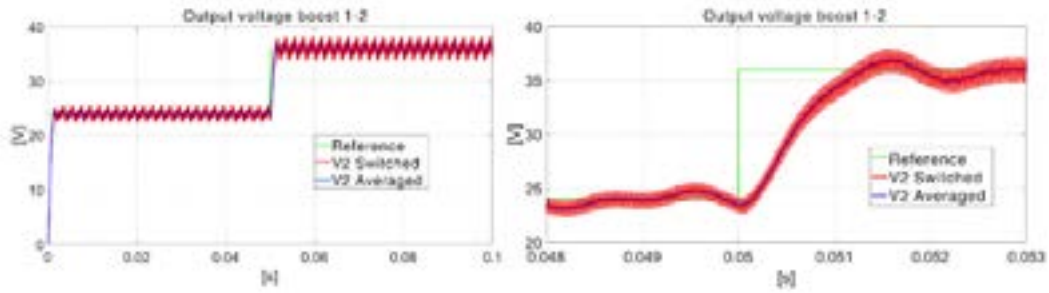

Figure 11. Comparison of the output voltage for $Boost_{1-2}$ operating mode (Switched converter circuit model vs. averaged and linearized canonical circuit model)

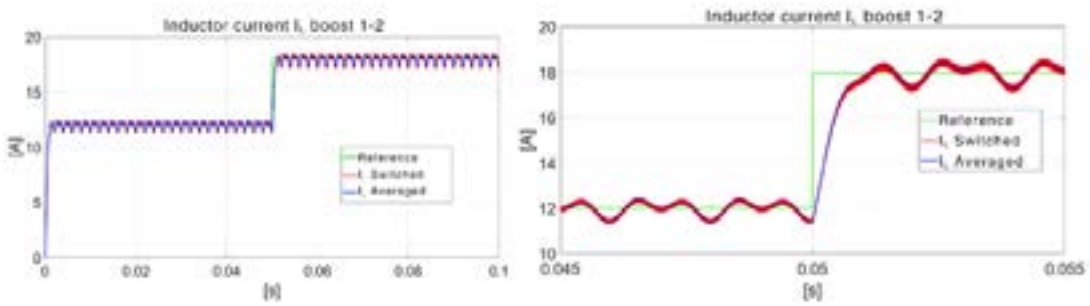

Figure 12. Comparison of the inductor current for the Boost1-2 operating mode (Switched converter circuit model vs. Averaged and linearized canonical circuit model)

Similarly, the $Buck_{2-1}$ mode of operation (reverse power flow) was analyzed. The results are shown in Figures 13 and 14. Comparisons of the output voltage (Figure 13) and inductor current (Figure 14) confirmed the validity of the model. The transient behavior exhibited an accurate dynamic representation of the bidirectional canonical model.

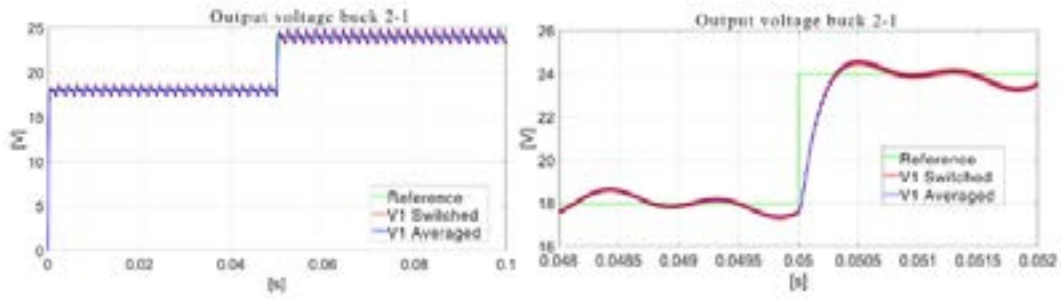

doi: 10.25100/iyc.v28i2.15590

Figure 13. Output voltage comparison for $Buck_{2\text{-}1}$ operating mode (Switched converter circuit model vs. Averaged and linearized canonical circuit model)

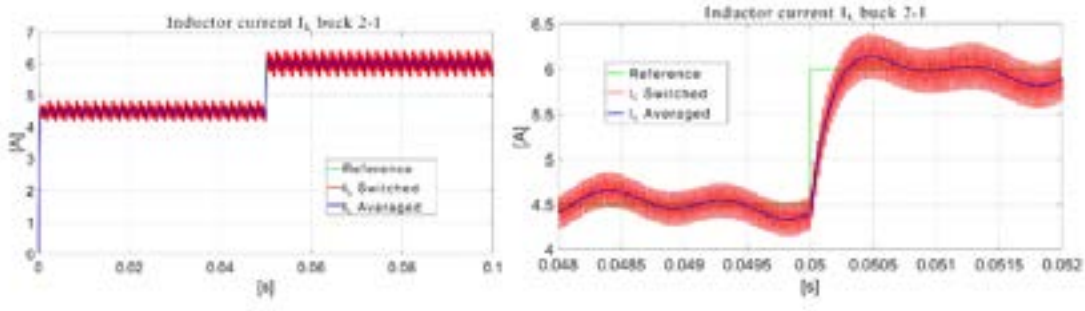

Figure 14. Comparison of the current through the inductor for $Buck_{2\text{-}1}$ operation mode (Switched converter circuit model vs. Averaged and linearized canonica circuit model)

The simulation results verified that the canonical bidirectional model enables an accurate representation of the low-frequency converter dynamics in its operating modes, making it a suitable tool for the design and analysis of control systems.

Discussion

Simulation times are extensive for full switching models due to inherent nonlinear dynamics. The average approximation extracts the low-frequency dynamics and the steady-state circuit response. A single canonical structure integrates the four operating modes (Buck1-2, Boost1-2, Buck2-1, and Boost2-1). This unified representation covers electric mobility applications with regenerative braking and battery energy storage systems. Classical frequency-domain analysis tools, such as Bode plots and root locus method, apply directly to the developed model for feedback controller design.

Conclusions

A unified circuit structure defines the cascaded buck-boost bidirectional DC/DC converter dynamics across four operating modes, removing the necessity of independent models for each power flow direction. Standard control theory tools including Bode plots and root loci apply directly to the canonical structure for feedback system design, as the averaged model captures the required low-frequency dynamics while omitting high-frequency ripples.

Direct evaluation against the switched equivalent circuit shows the canonical model accurately represents system dynamics regarding current, voltage, and transient response. The steady-state error between averaged signals and the canonical outputs remains below 1%. Observed transient deviations relate directly to the linearization and averaging assumptions. Consequently, these equations provide a basis for dynamic analysis and control synthesis in charging and discharging scenarios for energy storage systems and electric vehicles.

doi: 10.25100/iyc.v28i2.15590

CrediT authorship contribution statement

Conceptualization - Ideas: Oscar Olarte Ortiz, María Alejandra Mantilla, Javier Enrique Solano Martínez. Data curations: Oscar Olarte Ortiz, María Alejandra Mantilla. Formal analysis: Oscar Olarte Ortiz, María Alejandra Mantilla. Investigation: Oscar Olarte Ortiz, María Alejandra Mantilla, Javier Enrique Solano Martínez. Methodology: Oscar Olarte Ortiz, María Alejandra Mantilla, Javier Enrique Solano Martínez. Project Management: Oscar Olarte Ortiz, María Alejandra Mantilla, Javier Enrique Solano Martínez. Resources: Oscar Olarte Ortiz, María Alejandra Mantilla, Javier Enrique Solano Martínez. Software: Oscar Olarte Ortiz, María Alejandra Mantilla. Supervision: María Alejandra Mantilla, Javier Enrique Solano Martínez. Validation: Oscar Olarte Ortiz, María Alejandra Mantilla. Writing - original draft - Preparation: Oscar Olarte Ortiz, María Alejandra Mantilla, Javier Enrique Solano Martínez. Writing - revision and editing -Preparation: Oscar Olarte Ortiz, María Alejandra Mantilla, Javier Enrique Solano Martínez.

Financiación: yes, Universidad Industrial de Santander.

Conflict of interest: does not declare. Ethical aspect: does not declare.

References

1. Schiller PL, Kenworthy JR. An introduction to sustainable transportation: Policy, planning and implementation: Second edition. An Introduction to Sustainable Transportation: Policy, Planning and Implementation: Second Edition (Internet). Taylor and Francis; 2017 (cited 2025 Dec 17);1–420.

https://doi.org/10.4324/9781315644486

2. Chapman L. Transport and climate change: a review. J Transp Geogr (Internet). Pergamon; 2007 (cited 2025 Dec 17);15:354–67.

https://doi.org/10.1016/J.JTRANGEO.2006.11.008

3. McBain B, Lenzen M, Albrecht G, Wackernagel M. Reducing the ecological footprint of urban cars. Int J Sustain Transp (Internet). Taylor and Francis Ltd.; 2018 (cited 2025 Dec 17);12:117–27.

https://doi.org/10.1080/15568318.2017.1336264

4. Ji S, Cherry CR, Bechle MJ, Wu Y, Marshall JD. Electric Vehicles in China: Emissions and Health Impacts. Environ Sci Technol (Internet). American Chemical Society; 2012 (cited 2025 Dec 17);46:2018–24.

https://doi.org/10.1021/ES202347Q

5. Behrendt F. Why cycling matters for electric mobility: towards diverse, active and sustainable e-mobilities. Mobilities (Internet). Routledge; 2018 (cited 2025 Dec 17);13:64–80.

https://doi.org/10.1080/17450101.2017.1335463

6. Alli G, Formentin S, Savaresi SM. On the suitability of EPACs in urban use. IFAC Proceedings Volumes (Internet). Elsevier; 2010 (cited 2025 Dec 17);43:277–84.

doi: 10.25100/iyc.v28i2.15590

https://doi.org/10.3182/20100913-3-US-2015.00096

7. Saeseiw C, Pongpri K, Kaewchum T, Somkun S, Pachanapan P. Power Management for V2G and V2H Operation Modes in Single-Phase PV/BES/EV Hybrid Energy System. World Electric Vehicle Journal 2025, Vol 16, (Internet). Multidisciplinary Digital Publishing Institute; 2025 (cited 2026 Jan 22);16.

https://doi.org/10.3390/WEVJ16100580

8. Wang J, Wang B, Zhang L, Wang J, Shchurov NI, Malozyomov B V. Review of bidirectional DC–DC converter topologies for hybrid energy storage system of new energy vehicles. Green Energy and Intelligent Transportation. Elsevier B.V.; 2022;1. https://doi.org/10.1016/j.geits.2022.100010

9. Panchanathan S, Vishnuram P, Rajamanickam N, Bajaj M, Blazek V, Prokop L, et al. A Comprehensive Review of the Bidirectional Converter Topologies for the Vehicle-to-Grid System. Energies 2023, Vol 16, (Internet). Multidisciplinary Digital Publishing Institute; 2023 (cited 2026 Jan 22);16.

https://doi.org/10.3390/EN16052503

10. Lin CH, Liu HW, Wang CM. Design and implementation of a bi-directional power converter for electric bike with charging feature. Proceedings of the 2010 5th IEEE Conference on Industrial Electronics and Applications, ICIEA 2010 (Internet). 2010 (cited 2025 Dec 17);538–43.

https://doi.org/10.1109/ICIEA.2010.5517092

11. Sousa DM, Costa Branco PJ, Dente JA. Electric bicycle using batteries and supercapacitors. 2007 European Conference on Power Electronics and Applications, EPE (Internet). 2007 (cited 2025 Dec 17);

https://doi.org/10.1109/EPE.2007.4417425

12. Somchaiwong N, Ponglangka W. Regenerative power control for electric bicycle. 2006 SICE-ICASE International Joint Conference (Internet). 2006 (cited 2025 Dec 17);4362–5.

https://doi.org/10.1109/SICE.2006.314654

13. Weng X, Xiao X, He W, Zhou Y, Shen Y, Zhao W, et al. Comprehensive comparison and analysis of non-inverting buck boost and conventional buck boost converters. The Journal of Engineering. Institution of Engineering and Technology (IET); 2019;2019:3030–4.

https://doi.org/10.1049/JOE.2018.8373

14. Abdel-Rahim O, Chub A, Blinov A, Vinnikov D, Peftitsis D. An Efficient Non-Inverting Buck-Boost Converter with Improved Step Up/Down Ability. Energies 2022, Vol 15, (Internet). Multidisciplinary Digital Publishing Institute; 2022 (cited 2026 Jan 22);15.

https://doi.org/10.3390/EN15134550

15. Kunstbergs N, Hinz H, Schofield N, Roll D. Efficiency Improvement of a Cascaded Buck and Boost Converter for Fuel Cell Hybrid Vehicles with Overlapping Input and Output Voltages. Inventions

doi: 10.25100/iyc.v28i2.15590

2022, Vol 7, (Internet). Multidisciplinary Digital Publishing Institute; 2022 (cited 2026 Jan 22);7.

https://doi.org/10.3390/INVENTIONS7030074

16. Tong Y, Salhi I, Wang Q, Lu G, Wu S. Bidirectional DC-DC Converter Topologies for Hybrid Energy Storage Systems in Electric Vehicles: A Comprehensive Review. Energies 2025, Vol 18, (Internet). Multidisciplinary Digital Publishing Institute; 2025 (cited 2026 Jan 22);18.

https://doi.org/10.3390/EN18092312

17. Nisha KS, Gaonkar DN. Model predictive control of three level buck/boost converter for bipolar DC microgrid applications. 2019 IEEE 16th India Council International Conference, INDICON 2019 - Symposium Proceedings (Internet). Institute of Electrical and Electronics Engineers Inc.; 2019 (cited 2026 Jan 22); https://doi.org/10.1109/INDICON47234.2019.9029051

18. Narula S, Corradini L, Maksimovic D. Unified Sliding-Mode Control of Non-Inverting Buck-Boost Converters. 2023 IEEE 24th Workshop on Control and Modeling for Power Electronics, COMPEL 2023 (Internet). Institute of Electrical and Electronics Engineers Inc.; 2023 (cited 2026 Jan 22);

https://doi.org/10.1109/COMPEL52896.2023.10220975

19. Andleeb M, Khan KL, Hussain S, Iqbal SJ. Non-Linear Modeling and Control of DC-DC Buck and Boost Converters For EV Application. 2022 1st International Conference on Sustainable Technology for Power and Energy Systems, STPES 2022 (Internet). Institute of Electrical and Electronics Engineers Inc.; 2022 (cited 2026 Jan 22);

https://doi.org/10.1109/STPES54845.2022.10006486

20. A. Elbaset A, Hassan MS. Small-Signal MATLAB/Simulink Model of DC–DC Buck Converter. Design and Power Quality Improvement of Photovoltaic Power System (Internet). Springer International Publishing; 2017 (cited 2025 Dec 17);97–114.

https://doi.org/10.1007/978-3-319-47464-9_5

21. Erickson RW, Maksimovic D. Fundamentals of Power Electronics, Third Edition. Fundamentals of Power Electronics, Third Edition. Springer International Publishing; 2020;1–1084.

https://doi.org/10.1007/978-3-030-43881-4/COVER

22. Da Silva ERC, Fernandes DA, De MacEdo AKP, Marcus N. Lima A. Signal-Flow Graph Modeling and Control of the DC-DC Multilevel Boost Converter. 2022 14th Seminar on Power Electronics and Control, SEPOC 2022 (Internet). Institute of Electrical and Electronics Engineers Inc.; 2022 (cited 2026 Jan 22); https://doi.org/10.1109/SEPOC54972.2022.9976417

23. Maksimović D, Zane R. Small-signal discrete-time modeling of digitally controlled DC-DC converters. Proceedings of the IEEE Workshop on Computers in Power Electronics, COMPEL (Internet). 2006 (cited 2026 Jan 22);231–5.

https://doi.org/10.1109/COMPEL.2006.305680

24. Choi B. Pulsewidth Modulated DC-to-DC Power Conversion: Circuits, Dynamics, Control, and DC

doi: 10.25100/iyc.v28i2.15590

Power Distribution Systems, Second Edition. Pulesewidth Modulated DC-to-DC Power Conversion: Circuits, Dynamics, Control, and DC Power Distribution Systems, Second Edition (Internet). wiley; 2021 (cited 2025 Dec 17);1–692.

https://doi.org/10.1002/9781119454489

25. Mashinchi Mahery H, Babaei E. Mathematical modeling of buck–boost dc–dc converter and investigation of converter elements on transient and steady state responses. International Journal of Electrical Power & Energy Systems (Internet). Elsevier; 2013 (cited 2025 Dec 17);44:949–63.

https://doi.org/10.1016/J.IJEPES.2012.08.035

26. Khuntia MR, Veerachary M. Analysis and Control of Pseudo Quadratic Buck-Boost Converter. 3rd International Conference on Energy, Power and Environment: Towards Clean Energy Technologies, ICEPE 2020 (Internet). Institute of Electrical and Electronics Engineers Inc.; 2021 (cited 2026 Jan 22);

https://doi.org/10.1109/ICEPE50861.2021.9404494

27. She Q, Jin J, Wang R. Modeling and Analysis of DC Impedance of Bidirectional AC/DC Converter with DC-Droop VSM Control Strategy. Proceedings - 2023 Power Electronics and Power System Conference, PEPSC 2023 (Internet). Institute of Electrical and Electronics Engineers Inc.; 2023 (cited 2026 Jan 22);18–25.

https://doi.org/10.1109/PEPSC58749.2023.10395418

28. Tuluhong A, Xu Z, Chang Q, Song T. Recent Developments in Bidirectional DC-DC Converter Topologies, Control Strategies, and Applications in Photovoltaic Power Generation Systems: A Comparative Review and Analysis. Electronics 2025, Vol 14, (Internet). Multidisciplinary Digital Publishing Institute; 2025 (cited 2026 Jan 22);14.

https://doi.org/10.3390/ELECTRONICS14020389

29. Middlebrook RD, Cuk S. A general unified approach to modelling switching-converter power stages. Institute of Electrical and Electronics Engineers (IEEE); 2015;18–34.

https://doi.org/10.1109/PESC.1976.7072895

doi: 10.25100/iyc.v28i2.15590